The Astrophysical Journal, 870:136 (13pp), 2019 January 10 https://doi.org/10.3847/1538-4357/aaf1c0

AGILE Detection of Gamma-Ray Sources Coincident with Cosmic Neutrino Events

F. Lucarelli[1,2], M. Tavani[3,4], G. Piano[3], A. Bulgarelli[5], I. Donnarumma[6], F. Verrecchia[1,2], C. Pittori[1,2], L. A. Antonelli[2], A. Argan[3], G. Barbiellini[7], P. Caraveo[8], M. Cardillo[3], P. W. Cattaneo[9], A. Chen[10], S. Colafrancesco[2,10], E. Costa[3,6], E. Del Monte[3], G. Di Cocco[5], A. Ferrari[11], V. Fioretti[5], M. Galli[5], P. Giommi[6], A. Giuliani[8], P. Lipari[12], F. Longo[13], S. Mereghetti[8], A. Morselli[14], F. Paoletti[3,15], N. Parmiggiani[5], A. Pellizzoni[16], P. Picozza[17], M. Pilia[16], A. Rappoldi[9], A. Trois[16], A. Ursi[3], S. Vercellone[18], and V. Vittorini[3]

(The *AGILE* Team)

[1] ASI Space Science Data Center (SSDC), Via del Politecnico snc, I-00133 Roma, Italy; fabrizio.lucarelli@ssdc.asi.it
[2] INAF—OAR, via Frascati 33, I-00078 Monte Porzio Catone (Roma), Italy
[3] INAF/IAPS—Roma, Via del Fosso del Cavaliere 100, I-00133 Roma, Italy; marco.tavani@iaps.inaf.it
[4] Univ. "Tor Vergata", Via della Ricerca Scientifica 1, I-00133 Roma, Italy
[5] INAF/IASF—Bologna, Via Gobetti 101, I-40129 Bologna, Italy
[6] Agenzia Spaziale Italiana (ASI), Via del Politecnico snc, I-00133 Roma, Italy
[7] Dipartimento di Fisica, Universita di Trieste and INFN, via Valerio 2, I-34127 Trieste, Italy
[8] INAF/IASF—Milano, via E.Bassini 15, I-20133 Milano, Italy
[9] INFN—Pavia, Via Bassi 6, I-27100 Pavia, Italy
[10] University of Witwatersrand, Johannesburg, South Africa
[11] CIFS, c/o Physics Department, University of Turin, via P. Giuria 1, I-10125 Torino, Italy
[12] INFN—Roma Sapienza, Piazzale Aldo Moro 2, I-00185 Roma, Italy
[13] Dip. di Fisica, Universita di Trieste and INFN, Via Valerio 2, I-34127 Trieste, Italy
[14] INFN—Roma Tor Vergata, via della Ricerca Scientifica 1, I-00133 Roma, Italy
[15] East Windsor RSD, 25a Leshin Lane, Hightstown, NJ 08520, USA
[16] INAF—Osservatorio Astronomico di Cagliari, via della Scienza 5, I-09047 Selargius (CA), Italy
[17] INFN—Roma Tor Vergata, via della Ricerca Scientifica 1, I-00133 Roma, Italy
[18] INAF—Oss. Astron. di Brera, Via E. Bianchi 46, I-23807 Merate (LC), Italy

Received 2018 September 21; revised 2018 November 15; accepted 2018 November 15; published 2019 January 16

Abstract

The origin of cosmic neutrinos is still largely unknown. Using data obtained by the gamma-ray imager on board the *Astro-rivelatore Gamma a Immagini Leggero* (*AGILE*) satellite, we systematically searched for transient gamma-ray sources above 100 MeV that are temporally and spatially coincident with 10 recent high-energy neutrino IceCube events. We found three *AGILE* candidate sources that can be considered possible counterparts to neutrino events. Detecting three gamma-ray/neutrino associations out of 10 IceCube events is shown to be unlikely due to a chance coincidence. One of the sources is related to the BL Lac source TXS 0506+056. For the other two *AGILE* gamma-ray sources there are no obvious known counterparts, and both Galactic and extragalactic origin should be considered.

Key words: astronomical databases: miscellaneous – BL Lacertae objects: general – gamma rays: galaxies – gamma rays: general – neutrinos

1. Introduction

The discovery of a diffuse flux of cosmic neutrinos by the IceCube experiment (Aartsen et al. 2013, 2015) opened a new field of investigation in the context of neutrino astronomy (after the detections of the Sun and SN 1987a). Energetic neutrinos of energies above 10 TeV can be produced in astrophysical beam dumps, where cosmic rays are accelerated in regions near compact objects or in shock fronts, and interact via proton–proton (p–p) or proton–photon (p–γ) collisions with matter or radiation fields surrounding the central engine or within an ejected plasma flow (see Halzen 2017 for a review). High-energy gamma-ray emission above GeV is expected to be associated with these hadronic processes, with intensities that vary depending on source characteristics and environment (Mészáros 2017).

No significant clustering of neutrinos above the expected background has been observed so far from any of the current experiments after several years of observations (Aartsen et al. 2017a; Albert et al. 2017). Active galactic nuclei (AGNs) of the blazar category are considered the main cosmic neutrino source candidates (Mannheim 1995), although it has been suggested, based on average properties, that they contribute only to a fraction of the observed diffuse flux (Aartsen et al. 2017b). A contribution from other types of active galaxies (starburst galaxies, radio galaxies; Loeb & Waxman 2006; Becker Tjus et al. 2014; Tavecchio et al. 2018), galaxy clusters/groups (Murase et al. 2008; Kotera et al. 2009), AGN winds (Wang & Loeb 2016; Lamastra et al. 2017), and Galactic sources (supernovae remnants expanding in dense molecular clouds, microquasars, hidden compact objects; Bednarek 2005; Vissani 2006; Anchordoqui et al. 2014; Sahakyan et al. 2014; Ahlers et al. 2016) should also be considered.

Observation of transient gamma-ray emission, spatially and temporally compatible with the IceCube neutrinos, is then crucial to identify their electromagnetic (EM) counterparts. Since 2016 April, the IceCube Collaboration has been alerting the astronomical community almost in real time whenever a single-track high-energy starting event (HESE) or an extremely high-energy (EHE) through-going track event, with an energy higher than several hundred TeV, is detected (Aartsen et al. 2017c). The implementation of the IceCube alert system with the possibility of fast follow-up observations by several space- and ground-based instruments allows a global search for this

Table 1
Three *AGILE* QL Detections Close in Time and Space to IceCube HESE/EHE Neutrinos

AGILE Source	IceCube Event	T_0 (MJD)	R.A. (J2000) (deg)	Decl. (J2000) (deg)	$F_\gamma(E > 100$ MeV) $\times 10^{-6}$ (ph cm^{-2} s^{-1})	Δt (days)	FAR	P_i Post-trial
A	IC-160731	57600.079	214.544	−0.3347	(1.8 ± 0.7)	−2.0	5.9×10^{-4}	2.0×10^{-3}
B	IC-170321	57833.314	98.3	−15.02	(1.5 ± 0.6)	−2.2	1.5×10^{-3}	5.7×10^{-3}
C	IC-170922	58018.871	77.43	5.72	(1.7 ± 0.7)	−2.8	1.0×10^{-3}	5.0×10^{-3}

Note. Columns 2–5 show the main parameters of the corresponding IceCube event (event ID, neutrino event time T_0, best-fit reconstructed centroid position in equatorial coordinates). Columns 6–9 show, respectively, the *AGILE* gamma-ray flux (above 100 MeV) estimated over the QL 2 day integration time bin, the distance in time Δt from the QL detection centroid, the false alarm rate (FAR) expected for each detection (see Appendix A for details of the *AGILE* FAR estimate.), and the corresponding post-trial false alarm probability P_i.

association. On 2017 September a first significant association (at the level of 3σ) was announced: the gamma-ray flaring blazar of the BL Lac class, TXS 0506+056, was identified as a likely EM counterpart to the IceCube event IC-170922 (Aartsen et al. 2018a). Furthermore, from the analysis of archival data, an excess of very high-energy (VHE) neutrinos from the direction of the same source has been also detected in 2014/2015 (Aartsen et al. 2018b). TXS 0506+056 is thus suggested as the first extragalactic neutrino point-like source ever detected.

We report here on a systematic search for *Astro-rivelatore Gamma a Immagini Leggero* (*AGILE*) transient gamma-ray counterparts to the IceCube HESE/EHE events announced through the GCN/AMON system. The paper is organized as follows: in Section 2 we present the results of the systematic search for gamma-ray sources, in coincidence with neutrino events, automatically detected by the *AGILE* Quick Look (QL) transient detection system. The level of *AGILE*/IceCube correlation for some significant gamma-ray detections found in the search is evaluated, estimating the probability to be accidental using the *AGILE* false alarm rate (FAR) computed through the method discussed in Appendix A. In Section 3, we further investigate the common *AGILE*/IceCube detections, and we explore the possible EM counterpart candidates using the cross-catalog search tools available from the ASI Space Science Data Center.[19] Finally, in Section 4, we discuss the astrophysical implications of the *AGILE* observations.

2. The *AGILE* Satellite Search for Gamma-Ray Counterparts to IceCube Neutrino Events

The *AGILE* satellite monitors cosmic gamma-ray sources in the energy range from 30 MeV to 30 GeV (Tavani et al. 2009). Since 2009 November, the satellite has been scanning the whole sky in spinning mode, being an all-sky detector for transient gamma-ray sources capable of exposing about 80% of the whole sky at any given time with good sensitivity and angular resolution to gamma-rays above 100 MeV.

In this observing mode, at the end of 2016 July, the main instrument onboard of the satellite, the gamma-ray imager GRID, detected a gamma-ray transient (AGL J1418+0008) spatially and temporally consistent with the IceCube event IC-160731 (Lucarelli et al. 2017b). This detection was the result of the automatic and QL search for gamma-ray transients above 100 MeV, performed daily over predefined 2 day integration time-bins of *AGILE*-GRID data (Bulgarelli et al. 2014).

Motivated by this first detection, we have explored the *AGILE* QL database to search for other transient gamma-ray detections with the following characteristics: (1) a centroid positionally compatible, within the *AGILE* angular resolution, with the reconstructed arrival directions of the IceCube HESE/EHE neutrino events, and (2) temporally occurring within a fixed search time window around the neutrino event time T_0. Since 2016 April, a total of 13 neutrino events have been made public[20] (see Appendix B for the complete list); 10 events survive additional checks by the IceCube team. In this paper, we consider these 10 events as the basis for our study.

Typical IceCube HESE/EHE error circles are of order of 1° in radius, and the mean *AGILE* angular resolution measured from in-flight and calibration data is ∼1.°5 in the energy range 100 MeV–1 GeV (Sabatini et al. 2015). Based on this, we have tried three values for the database search radius around the 10 IceCube input sky positions (1.°0, 1.°5, and 2.°0), which are within the range of the *AGILE* point-spread function (PSF). Concerning the time window of interest, the astrophysics and timescales of the phenomena related to the emission of these EHE neutrinos and their likely correlated gamma-ray emission are still uncertain. Thus, based on the typical *AGILE* sensitivity to a transient gamma-ray source, we consider the *AGILE* QL detection *temporally* consistent with the neutrino event *if* it occurs within a time interval of plus/minus 4 days around T_0.

From the QL database mining, using the optimized 1.°5 search cone radius, we found three significant *AGILE* detections which satisfy the temporal and spatial association criteria defined above in correspondence with the three IceCube events: IC-160731, IC-170321, and IC-170922. From now on, we will indicate the corresponding three *AGILE* detections as *AGILE* Source A, Source B, and Source C. Table 1 shows the details of the three *AGILE* QL detections, along with the main parameters of the closest IceCube detection (event ID, neutrino event time T_0, and best-fit reconstructed centroid position in equatorial coordinates). In all cases, the gamma-ray position is within the *AGILE* angular resolution (1.°5) from the best-fit IceCube reconstructed arrival direction. The table also shows the time difference Δt between T_0 and the center of the 2 day integration interval of the closest QL detection, and the corresponding gamma-ray flux above 100 MeV evaluated by means of the *AGILE* maximum likelihood (ML) algorithm (Bulgarelli et al. 2012).

The first *AGILE*/IceCube event in Table 1 is AGL J1418+0008, whose detection was already reported in Lucarelli et al. (2017b). *AGILE* Source B is reported here for the first time: this

[19] http://www.ssdc.asi.it

[20] https://gcn.gsfc.nasa.gov/amon_hese_events.html and https://gcn.gsfc.nasa.gov/amon_ehe_events.html.

detection, with a gamma-ray flux above 100 MeV of $F = (1.5 \pm 0.6) \times 10^{-6}$ ph cm^{-2} s^{-1}, is temporally close (2 days prior) to the IceCube event that occurred on 2017 March 21 (Blaufuss 2017a). The last one, Source C, corresponds to the most recent IceCube-170922A event and is consistent with the gamma-ray activity from the blazar TXS 0506+056 as reported in Aartsen et al. (2018a). We notice that all three events with an *AGILE* nearby source detection belong to the EHE event class with track-like characteristics (Aartsen et al. 2017c) (see also Table 4 in Appendix B).

All three QL detections are confirmed using the standard *AGILE* analysis (Bulgarelli et al. 2012), applying additionally a more stringent cut on the Earth albedo contamination.[21] Figure 1 shows: in the left panel, the *AGILE*-GRID gamma-ray lightcurves above 100 MeV around T_0 for each of the three sources; in the right panel, the gamma-ray intensity maps above 100 MeV corresponding to the detection found near T_0.

The standard *AGILE* data analysis indicates that in all cases the peak gamma-ray emission is similarly observed within 1–2 days from T_0. For Sources B (IC-170321) and C (IC-170922), weak gamma-ray emission is also observed over longer integration timescales that include T_0. In particular, for the new Source B an integration of 15 days, starting from 2017 March 15 (12:00 UT), shows a detection above 4σ with a flux $F(E > 100\ \mathrm{MeV}) = (4.6 \pm 1.6) \times 10^{-7}$ ph cm^{-2} s^{-1}. The *AGILE* centroid has Galactic coordinates $(l, b) = (224.59, -10.53) \pm 0.42$ (deg) (95% stat. c.l.) $\pm$ 0.1 (deg) (syst.) (R.A., decl. (J2000) = (98.58, −15.08) (deg)), and is fully compatible with the IceCube centroid (see Figure 2).

2.1. Post-trial False Alarm Probability

To evaluate the probability that each of these three gamma-ray sources is associated with the neutrino events by chance, we first evaluated the FAR for an *AGILE* QL detection per unit time δt and per unit solid angle $\delta\Omega$. As the unit time δt, we assumed the standard integration time of the QL maps ($\delta t = 2$ days). For $\delta\Omega$, we assumed the solid angle subtended by a cone with half-aperture matching the standard circular radius of 1.°5 used in the database search ($\delta\Omega \simeq 2.15 \times 10^{-3}$ sr).[22] We then estimated the post-trial false alarm probability P_i of a random occurrence in *space* and *time* of a neutrino and a gamma-ray transient event separated by an interval Δt and by the solid angle $\Delta\Omega$ (corresponding to the angular distance $\Delta\theta$) as (Connaughton et al. 2016)

$$P_i = N_i * \mathrm{FAR}(\geqslant\sqrt{\mathrm{TS}}) * \Delta\mathrm{t} * (1 + \ln(\Delta T/\delta t)) * \Delta\Omega \quad (1)$$

where N_i is the number of trials for a symmetric time window, $\mathrm{FAR}(\geqslant\sqrt{\mathrm{TS}})$ is the FAR per 2 day map and per unit solid angle for *AGILE* detections above a given significance $\sqrt{\mathrm{TS}}$,[23] Δt is the absolute time difference between the QL detection centroid and T_0, and ΔT is the one-sided time interval over which the search is done (set beforehand to $\Delta T = 4$ days). We have assumed a spatial coincidence whenever the centroids of the *AGILE*/IceCube detections are within an angular distance $\Delta\theta = 1.°5$, so that in our case $\Delta\Omega \equiv \delta\Omega$.

Since the gamma-ray detection strategy we adopted is fully automated,[24] and there is no refined analysis around T_0 , the trial factor N_i takes into account only the choice of the symmetric window around T_0 and is thus equal to 2.

The last two columns of Table 1 show, respectively, the FAR (per 2 day map and per unit solid angle) and the corresponding post-trial false alarm probability P_i of a random coincidence with the IceCube neutrinos for each of the three QL detections. For each *AGILE* source, the post-trial chance correlation is of the order of 10^{-3}.

Given this basic information, we then proceed to calculate the joint post-trial probability to observe three gamma-ray sources out of 10 neutrino alerts over the period of the active IceCube alert system, as

$$P_{\mathrm{joint}}(\text{post-trial}) = 1 - (1 - P_A * P_B * P_C)^N \quad (2)$$

where the number of global trials N is given by the product of two contributions: the total number of IceCube HESE/EHE events considered (equal to 10), and the number (equal to three) of optimizations of the search radius of the gamma-ray error boxes. We therefore determine the joint *post-trial chance probability* to be

$$P_{\mathrm{joint}}(\text{post-trial}) = 1.7 \times 10^{-6} \quad (3)$$

which corresponds to a number of Gaussian equivalent one-sided standard deviations of approximately 4.7σ.

Alternatively, assuming an average post-trial false alarm probability $p = 4.0 \times 10^{-3}$ for a typical gamma-ray source, we can use a binomial probability distribution to estimate the probability to observe three *AGILE* gamma-ray counterparts out of 10 IceCube events in the whole sky. This results in a probability of the order of 7.5×10^{-6} (one-sided 4.3σ).

3. Possible EM Counterparts to the IceCube Events and the Sources A, B and C Detected by *AGILE*

3.1. AGILE *Source A/IC-160731 Event*

The first IceCube HESE/EHE event, compatible and temporally close to an automatic *AGILE* QL detection, occurred on 2016 July 31 (T_0 = MJD 57600.079). The event and the possible *AGILE* gamma-ray counterpart (AGL J1418 +0008) were extensively studied in Lucarelli et al. (2017b). The EM follow-up of the event did not reveal any transient sources within the IceCube error circle. Using the online SSDC *SkyExplorer* tool[25] and the ASI *Open Universe* web portal,[26] in this work we have performed a new search for possible known EM counterparts within the common *AGILE*/IC-170321 confidence error regions. Figure 3, left panel, shows the result of a query for cataloged radio, X-ray, and gamma-ray sources within 60 arcmin from the IceCube centroid, placed at R.A., decl. (J2000) = (214.544, −0.3347 deg). The 60 arcmin search radius encompasses the whole IC-160731 error circle and also covers most of the 95% c.l. error circle of the *AGILE* Source A detection (see Figure 1, upper panel).

[21] For comparison, the predefined QL maps are generated with a looser Earth albedo cut of 80°.

[22] See Appendix A for details of the FAR computation.

[23] See Bulgarelli et al. (2012) for the definition of an *AGILE* detection based on the value of the test statistic obtained after the application of the *AGILE* multi-source ML algorithm.

[24] The start and stop times of the 2 day integration have been defined a priori since the start of the spinning observation mode.

[25] https://tools.ssdc.asi.it

[26] http://www.openuniverse.asi.it

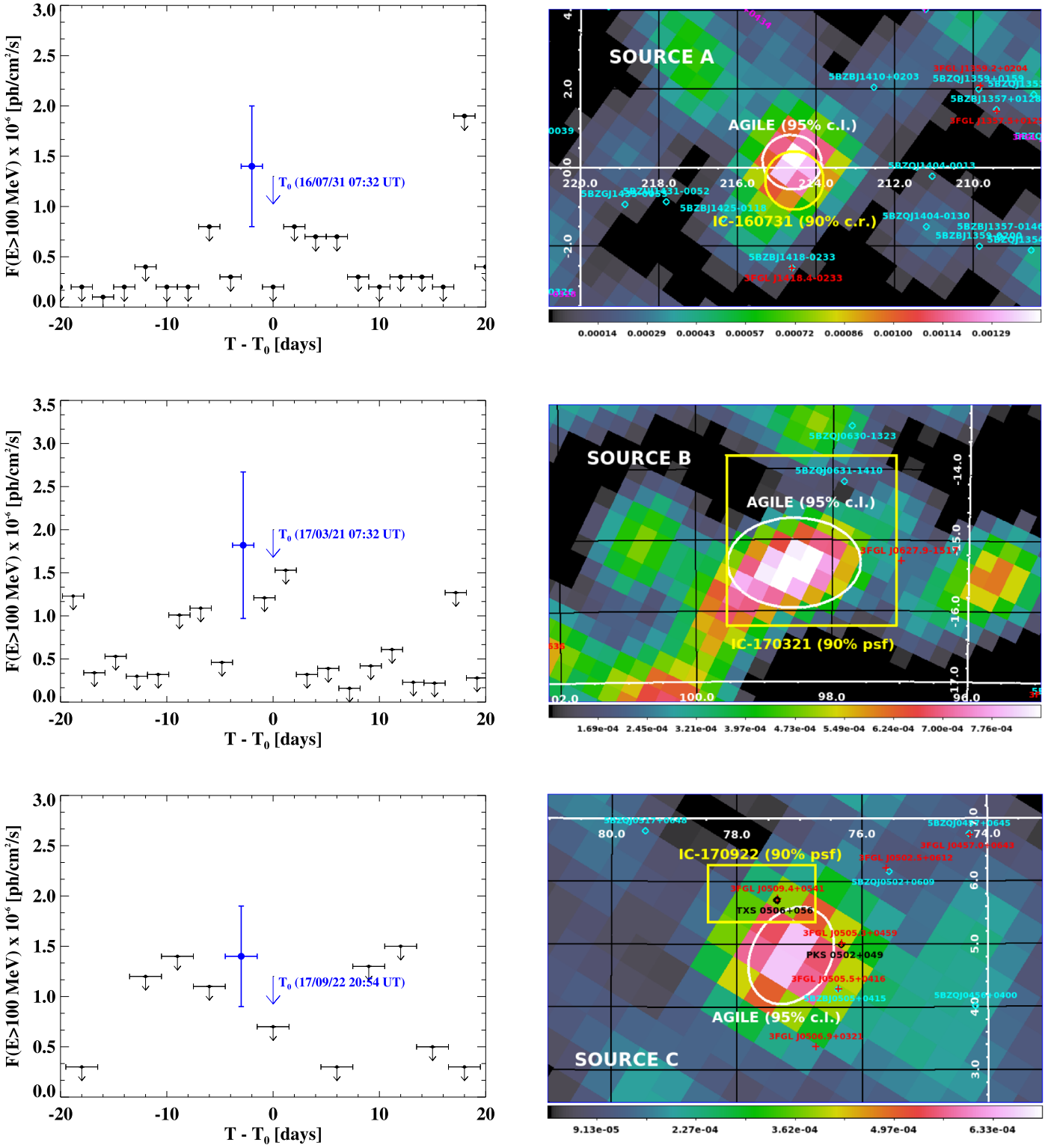

Figure 1. Results of the *AGILE*-GRID standard analysis for the three Sources A (upper panel), B (middle panel) and C (lower panel) of Table 1. Left panels: gamma-ray lightcurves above 100 MeV around the IceCube T_0. Right panels: maps in equatorial coordinates (J2000) of gamma-ray intensity above 100 MeV in (ph cm^{-2} s^{-1} sr^{-1}) corresponding to the gamma-ray detection before T_0 shown on the left. The *AGILE* 95% confidence level (c.l.) location contours are shown in white; the IceCube error boxes or circles are shown in yellow. A systematic error of 0.°1 should be added to each *AGILE* source determination. The positions of the classified AGNs from the BZCAT Catalog (Massaro et al. 2015) and the *FERMI*-LAT 3FGL gamma-ray sources (Acero et al. 2015) are shown in cyan and red, respectively.

The sky region within the gamma-ray and neutrino error regions does not show any obvious EM counterpart, in particular, neither known gamma-ray sources nor known AGN blazars appear within the search radius chosen for the query. The X-ray source 1RXS J141658.001449 (labeled as 1 in Figure 3) was suggested by Lucarelli et al. (2017b) as a potential high-peaked BL Lac (HBL) AGN blazar. Nevertheless, a dedicated *Swift*-XRT observation taken some months

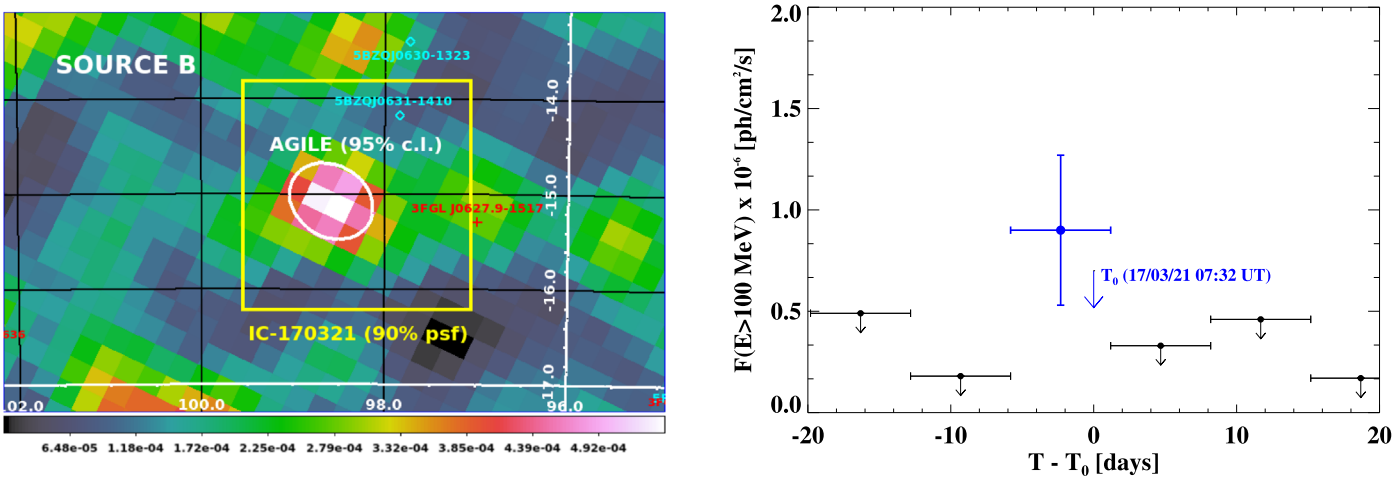

Figure 2. Left panel: *AGILE*-GRID intensity maps, in (ph cm^{-2} s^{-1} sr^{-1}) and equatorial coordinates (J2000), centered at the position of the IceCube event IC-170321, over a long integration time of 15 days around T_0 ($(T_0 - 6; T_0 + 11)$ days). The *AGILE* 95% c.l. location contour obtained with the *AGILE* standard analysis is shown in white, the IceCube error box in yellow. Right panel: *AGILE*-GRID 7 day time bin gamma-ray lightcurve ($E > 100$ MeV) around T_0, obtained from the *AGILE* standard analysis performed at the IC-170321 position.

after the neutrino event time T_0, did not confirm any steady X-ray emission from this position, thus the former hypothesis could not be confirmed.

Five uncataloged X-ray sources were detected during the previous *Swift* target of opportunity (Lucarelli et al. 2017b): their positions are indicated by the blue crosses in Figure 3. One of them (source labeled as 2) is positionally consistent with the radio source NVSS J141746-001151 and the object SDSS J141746.65-001149.8, which is actually cataloged as star.

Interestingly this region shows the presence of several galaxy clusters (indicated by the black circles in Figure 3), which could host a possible AGN or a different class of powerful active sources that could be the origin of the IceCube neutrino and the gamma-ray transient emission detected by *AGILE*. In particular, based on its radio/X-ray positional association and flux intensity, one of the most interesting neutrino source candidates within this sky region is that labeled as 3 in Figure 3 (R.A., decl. (J2000) = 213.74038, −0.34967 deg). The radio and X-ray emissions are positionally consistent with the elliptical galaxy SDSS J141457.72-002058.6, whose broadband spectral properties resemble those typical of a high synchrotron peaked (HSP) blazar (see Figure 3, right panel).[27]

3.2. AGILE *Source B/IC-170321 Event*

The second IceCube HESE/EHE event, compatible and temporally close to an automatic *AGILE* QL detection, occurred on 2017 March 21 (T_0 = MJD 57833.314). The ML significance of the QL detection is slightly lower than the others but it is again confirmed through the standard *AGILE* analysis using a longer integration window around T_0, applying additionally a more stringent cut on the Earth albedo contamination.

The EM follow-up of the event did not reveal any transient source within the IceCube error box: in the high-energy gamma-ray band, *Fermi*-LAT placed a 95% c.l. upper limit (u.l.) above 100 MeV for point-like emission at the IceCube position over different time intervals near and before T_0, with the most stringent found to be 5.5×10^{-8} ph cm^{-2} s^{-1} in one week of exposure prior to T_0 (Buson et al. 2017).

In the hard X-ray/gamma-ray band, *INTEGRAL* and Konus-*Wind* reported an u.l. on burst-type emission over short time periods around T_0 (Savchenko et al. 2017; Svinkin et al. 2017). The *Swift*-XRT follow-up, with a seven-tile mosaic covering only 21% of the 90% error box on the refined IceCube localization, detected only one known X-ray source (1SXPS J063214.5-143300) at a flux level consistent with the cataloged value (Keivani 2017). Archival data from *Swift*-BAT[28] did not show any transient hard-X-ray emission at this position. No optical follow-up was reported for the event. We explored the All-Sky Automated Survey for SuperNovae transient web page[29] and the Palomar Transient Factory catalog[30] but did not find any transient optical emission within 1° from the IceCube centroid.

Using the online SSDC *SkyExplorer* tool (see footnote 25) and the ASI *Open Universe* web portal (see footnote 26), we searched also for this event a possible common EM counterpart for the IC-170321 neutrino and *AGILE* Source B. Figure 4 shows the result of a query for cataloged radio, X-ray, and gamma-ray sources within 90 arcmin from the IceCube centroid, which fully contains the *AGILE* Source B error circle. Labels from 1 to 10 in Figure 4 indicate the most interesting neutrino/gamma emitter candidates found in the search, based on their radio/X-ray positional association and flux intensity. Among them, we found two flat spectrum radio quasars (FSRQs), one 3FGL source, 3FGL J0627.9-1517, and three possible blazars of the HBL sub-class. Details of each of the 10 sources are reported in Table 2.

Assuming the HBL sub-class of blazars as one of the most promising neutrino emitter candidates (Padovani et al. 2016; Resconi et al. 2017), one of the most interesting source within the *SkyExplorer* search radius appears to be the 3FGL J0627.9-1517 source (#6 in Figure 4), which has been recently

[27] Indeed, this object has been recently included in the third edition of the extreme and HSP blazars catalog as 3HSP J141457.7-002058 (Chang et al. 2018).

[28] https://swift.gsfc.nasa.gov/results/transients/index.html
[29] http://www.astronomy.ohio-state.edu/asassn/transients.html
[30] http://irsa.ipac.caltech.edu/Missions/ptf.html

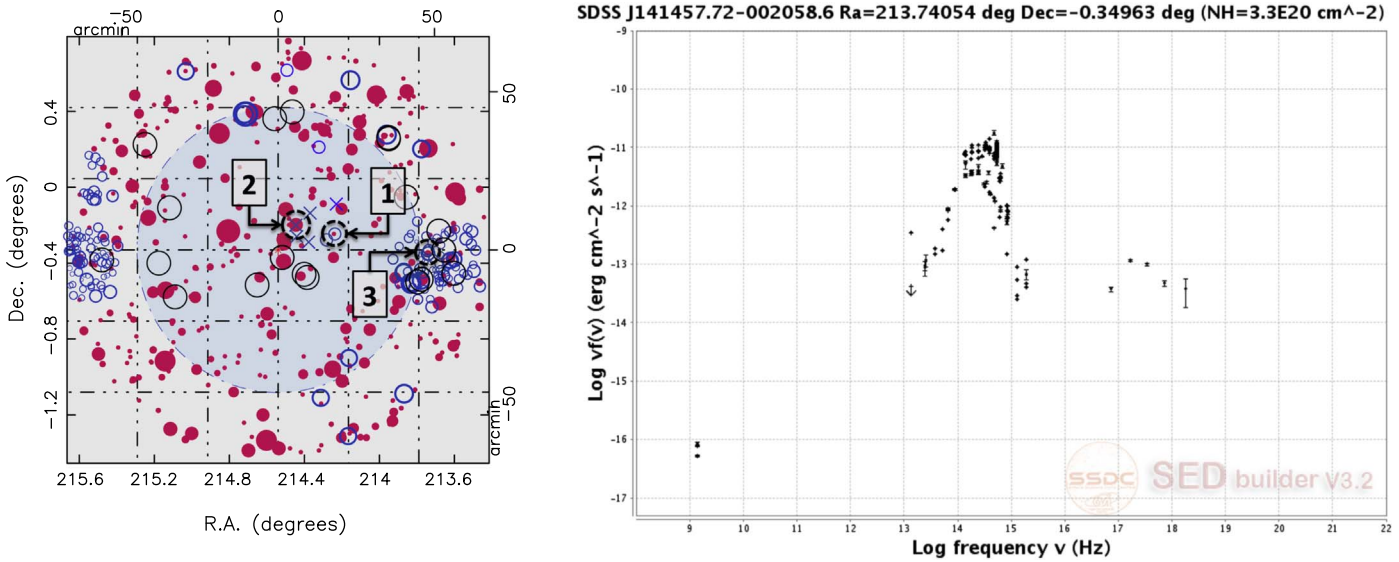

Figure 3. Left panel: R.A.–decl. sky map (J2000) obtained using the SSDC *SkyExplorer* tool (see footnote 25) and the ASI *Open Universe* tool (see footnote 26) showing known radio (red filled circles) and X-ray (open blue circles) sources within 60 arcmin from the IC-160731 centroid (R.A., decl. (J2000) = (214.544, −0.3347) deg). The blueish circular area represents the position uncertainty (90% c.r.) quoted by the IceCube Coll. for the IC-160731 event (see Table 4). The map also covers most of the 95% c.l. contour of the *AGILE* Source A (already known as AGL J1418+0008), centered at R.A., decl. (J2000) = (214.61, 0.13 deg). Black open circles are all known galaxy clusters from existing catalogs. Source intensities are related to the circle diameters. The source labeled as 1 was already studied in Lucarelli et al. (2017b). Blue crosses indicate the positions of five uncataloged X-ray sources detected during a dedicated *Swift* observation of source 1. The source labeled as 3 is a possible high-peaked BL Lac blazar candidate. Right panel: spectral energy density of the high-peaked BL Lac/high synchrotron peaked blazar candidate labeled as 3 in the figure on the left, obtained with archival data from radio to X-rays available at the SSDC.

classified as the HSP blazar 2WHSP J062753.2-151956 (Chang et al. 2017). The steady average 3FGL flux above 100 MeV for this source is below 2×10^{-8} ph cm^{-2} s^{-1}. The gamma-ray light curve above 1 GeV produced with the *Fermi*-LAT online data analysis tool available at SSDC,[31] with a 7 day binning, did not show any relevant activity in the six months around the neutrino event T_0, except for one small peak, appearing some days later it was not confirmed by a further analysis made with the official *Fermi* Science Tools (v10r0p5).[32]

3.3. AGILE *Source C/IC-170922 Event*

The first *AGILE* detection of a gamma-ray counterpart above 100 MeV consistent with the position of the neutrino event IC-170922 was first reported in Lucarelli et al. (2017a). Again, the detection initially appeared as result of the automatic QL daily processing, and was confirmed afterwards using the standard *AGILE* analysis. The EM follow-up triggered by the GCN Notice and the GCN Circular announcing the identification of an EHE neutrino event by IceCube (Kopper & Blaufuss 2017) allowed the identification of the blazar BL Lac TXS 0506+056 (also known as 5BZB J0509+0541; Massaro et al. 2015) as the likely counterpart of the IceCube event (Aartsen et al. 2018a).

Using GRID data with energies above 400 MeV in a time interval of three days close to the neutrino event T_0, we obtained a better positional agreement of the *AGILE* detection with the TXS 0506+059 source, contained within the IC-170922 error box (see Figure 5, left panel), which thus confirms the gamma-ray activity observed from the source during this period (Tanaka et al. 2017; Aartsen et al. 2018a).

As reported in Aartsen et al. (2018a), the source has been active in gamma-rays since a time several months before 2017 September. Figure 5, right panel, shows the *AGILE* gamma-ray lightcurve above 100 MeV from the beginning of 2017 August until the end of September, estimated on the TXS 0506+056 position. Superimposed is the corresponding *Fermi*-LAT curve (red points) obtained with the public analysis tool available at SSDC (see footnote 31), which shows a good agreement with the flaring activity detected by *AGILE*.[33]

A recent IceCube paper claimed a second excess of VHE neutrinos observed from the direction of TXS 0506+056 in the period from 2014 September to the beginning of 2015 (Aartsen et al. 2018b). The analysis of the *AGILE*-GRID data over this period around the TXS 0506+059 position shows a strong gamma-ray contribution from the near FSRQ source PKS 0502 +049 (1.°2 away), which was in a high flaring state at that epoch (Lucarelli et al. 2014; Ojha et al. 2014). Using *Fermi*-LAT data, Padovani et al. (2018) show that the gamma-ray emission from the TXS is particularly hard compared to the softer emission from the FSRQ, and becomes predominant only by selecting gamma-rays above the GeV. Indeed, our analysis also shows that the contribution from PKS 0502+049 above a few GeV becomes negligible but, due to the limited *AGILE* gamma-ray sensitivity above 1 GeV, we can set a flux u.l. $< 3.8 \times 10^{-8}$ ph cm^{-2} s^{-1} for $E > 1$ GeV (for a 95% c.l.) over the emission from the TXS 0506+056 during this period.

4. Discussion and Conclusions

We reported the results of the *AGILE* gamma-ray observations of the error regions of 10 IceCube HESE/EHE neutrino events announced since 2016 April through the GCN/AMON system.

[31] https://tools.asdc.asi.it/?&searchtype=fermi
[32] https://fermi.gsfc.nasa.gov/ssc/data/analysis/software/
[33] We notice that the *Fermi*-LAT fluxes estimated with the online tool can be overestimated up to a factor of 2.

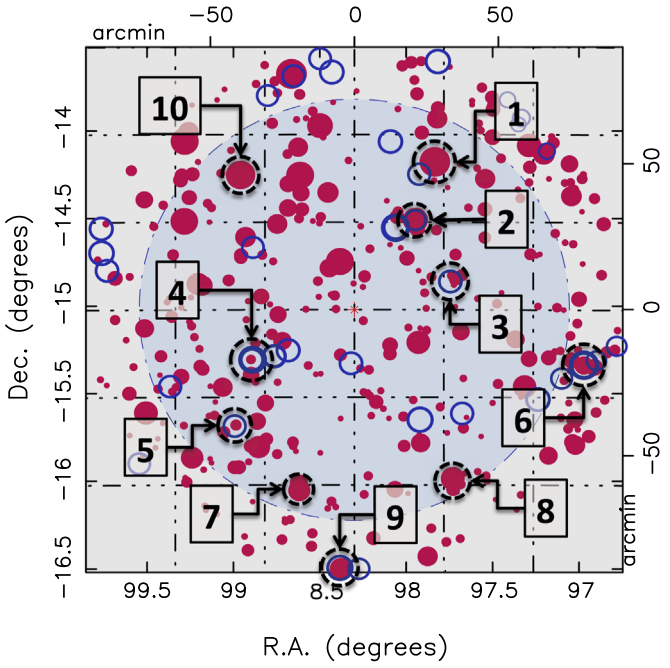

Figure 4. R.A.–decl. sky map (J2000) obtained using the SSDC *SkyExplorer* tool and the ASI *Open Universe* tool showing known radio, X-ray, and gamma-ray sources within 90 arcmin from the IC-170321 centroid (R.A.–decl. (J2000): 98.3, −15.02 (deg)). The blueish circular area represents the uncertainty (90% point-spread function) on the reconstructed neutrino arrival direction quoted by IceCube for the IC-170321 event (see Table 4). The map also covers the whole 95% c.l. error circle of *AGILE* Source B, centered at R.A., decl. (J2000) = (98.58, −15.08 deg). Radio (red filled circles) plus X-ray (open blue circles) sources are from existing catalogs. Possible common EM candidate counterparts are enclosed by black dashed circles and labeled from 1 to 10. Details of each candidate are reported in Table 2.

Mining the database of automated *AGILE*-GRID *QL* detections, determined on predefined 2 day integration maps, we found three significant gamma-ray detections above 100 MeV within 1°.5 from the IceCube best-fit centroids, and within 2 days from the neutrino event time T_0. The *AGILE* automatic detections, each of them with a significance at the level of 4σ estimated using the *AGILE* ML algorithm, are compatible in position and time with the three IceCube events IC-160731, IC-170321, and IC-170922, all of them classified as EHE.

We dubbed the three *AGILE* Sources A, B, and C. The global post-trial probability found in our study for the *AGILE*/IceCube chance correlation for three out of 10 events is quite low (around 4.7 Gaussian standard deviations), and significantly hints toward an astrophysical connection between the *AGILE* detections and the observed IceCube single-track events.

A direct correlation between gamma-rays and neutrinos from astrophysical sources is expected whenever hadronic emission mechanisms are at work. In a hadronic source scenario, we do expect comparable values of the gamma-ray/neutrino observed luminosities (Gaisser et al. 1995). We thus estimate the *AGILE* gamma-ray luminosities for each of the three Sources A, B, and C, and compare them with the corresponding neutrino luminosities, assuming a typical timescale of six months for neutrino production as a product of an underlying hadron acceleration and interaction (Aartsen et al. 2018a). With Sources A and B unidentified, we assume two values for their possible distance: 10 kpc (typical of a Galactic object), and redshift $z = 1$ (for an extragalactic object). For Source C, we make use of the TXS 0506+056 redshift, $z = (0.3365 \pm 0.0010)$, recently estimated by Paiano et al. (2018). For the calculation of the neutrino luminosities, we adopt the muon neutrino fluence value of 2.8×10^{-3} erg cm^{-2} estimated in Aartsen et al. (2018a), for which we would expect to detect one high-energy neutrino event with IceCube over its entire lifetime.[34]

Table 3 displays the gamma-ray energy density fluxes and luminosities above 100 MeV, estimated in a time interval of about ±1 week around T_0, and the neutrino luminosities estimated assuming a source active period of six months. Interestingly, for each of the three events we obtain similar values of the luminosities in gamma-ray and neutrinos. The observed power for the two adopted distances (assumed to be emitted isotropically), is typical of Galactic and extragalactic compact objects in the range of 10^{36} erg s^{-1} or 10^{47} erg s^{-1}, respectively.

In case of IC-170922A (Source C) we observed a significant temporal correlation between the neutrino event and the almost simultaneous gamma-ray activity in HE and VHE bands from the IBL/HBL BL Lac type of blazar TXS 0506+056 (Aartsen et al. 2018a). This is suggestive of this AGN sub-class of blazars being one of the main VHE neutrino emitters from hadronic processes. In the other two cases (A and B) there is no clear evidence of flaring activity from any known EM source inside the *AGILE*/IceCube common error circles. A search for possible EM counterparts within the common *AGILE*/IceCube error regions, initially focusing on the identification of unknown HBL/HSP blazar candidates, found no obvious blazar candidates for Source A, as discussed in Lucarelli et al. (2017b). A further investigation made in this work has identified a new possible HBL candidate, the elliptical galaxy SDSS J141457.72-002058.6. Regarding the gamma-ray Source B, presented in this paper for the first time, some potential HBL blazars are found within the uncertainty neutrino/gamma regions. Moreover, a *Fermi*-3FGL source, 3FGL J0627.9-1517, recently associated with an HSP blazar, is at the boundary of the 90% IceCube error box, although well outside the smaller AGILE error circle obtained on the longer integration around T_0 (see Figure 4).

Given the lack of clear blazar counterparts for Sources A and B, we are led to explore alternative explanations. Different classes of extragalactic sources, potentially hosting hadronic processes (bursts from radio galaxies, starburst galaxies, eruptions from AGN cores, etc.) might be invoked to explain the gamma/neutrino correlations for A and B. Furthermore, IceCube neutrino fluxes can be produced also by gamma-ray hidden sources for which the high matter/radiation density surrounding a central engine enhances the target matter for the p–p or p–γ absorption processes. This would result in an observable neutrino flux with a highly suppressed gamma-ray flux from neutral pion decay. The *AGILE* detections of gamma-ray sources near IC-160731 (Source A) and IC-170321 (Source B) indicate the possibility that, from time to time, under particularly favorable conditions the neutrino source may become transparent to MeV/GeV gamma-rays. Taking into account the optimized *AGILE* sensitivity to soft gamma-ray emission in the 100–400 MeV energy band, sources with softer spectra can also be considered. For example, in such a case of enhanced target density, we might expect to observe a soft

[34] A power-law neutrino spectrum is assumed in this estimation with an index equal to −2 between 200 TeV and 7.5 PeV (Aartsen et al. 2018a).

Table 2
Possible EM Candidate Counterparts for IC-170321 and the *AGILE* Source B Detected in the Days around T_0

ID	Catalog Name	R.A. (J2000) (deg)	Decl. (J2000) (deg)	Other Association	Source Class	Distance from IC-170321 Centroid (arcmin)
1	5BZQ J0631-1410	97.83429	−14.1755	CRATES J063119-141030	FSRQ	58
2	CRATES J063148-143042	97.94638	−14.50844	⋯	Possible IBL	37
3	PSZ2 G224.01-11.14	97.75250	−14.83520	⋯	Cluster of Galaxies	34
4	NVSS J063535-151813	98.89838	−15.30361	1RXS J063533.5-151817	Possible HBL	39
5	NVSS J063556-154038	98.98450	−15.67736	1RXS J063558.2-15410	Possible HBL	56
6	3FGL J0627.9-1517	96.9853	−15.29782	WHSP J062753.2-151956	HSP BL Lac	79
7	CRATES J063428-160239	98.6191	−16.0519	⋯	Flat spectrum radio source	65
8	CRATES J063053-155929	97.7306	−15.9829	⋯	Flat spectrum radio source	67
9	CRATES J063329-163020	98.38046	−16.5201	⋯	Possible HBL	89
10	PMN J0635-1415	98.95842	−14.25011	⋯	Flat spectrum radio source	60

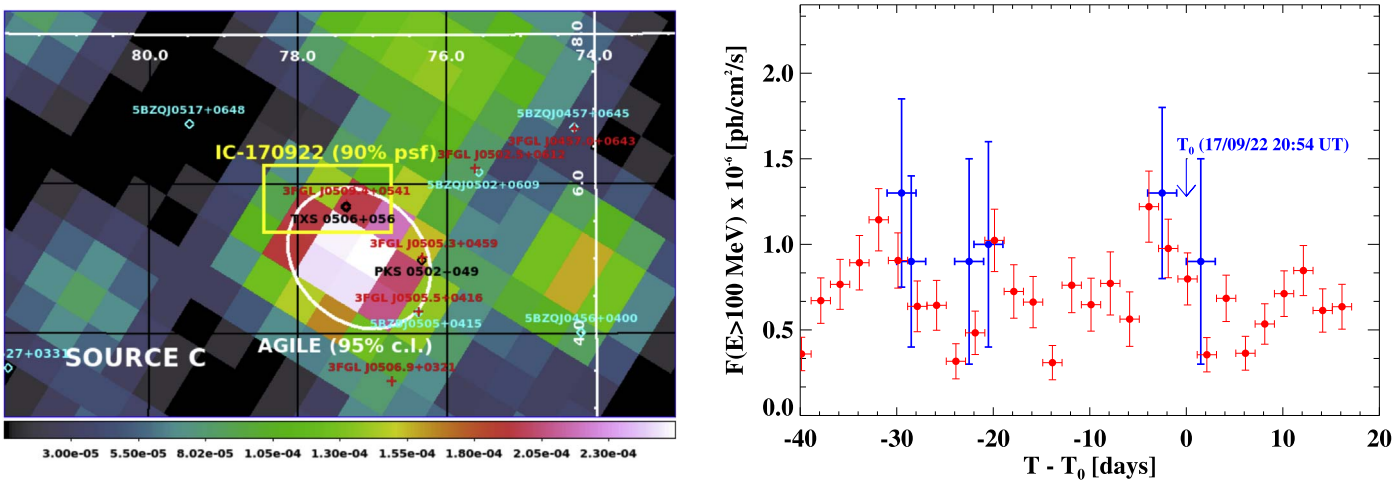

Figure 5. Left panel: *AGILE*-GRID intensity map above 400 MeV, in (ph cm^{-2} s^{-1} sr^{-1}) and equatorial coordinates (J2000), around the region of the TXS 0506+059 source, over the period ($T_0 - 4$; $T_0 - 1$) days. The *AGILE* 95% c.l. contour obtained with the *AGILE* standard analysis is shown in white; the IceCube error box (Kopper & Blaufuss 2017) is shown in yellow. The positions of the classified AGNs from the BZCAT Catalog (Massaro et al. 2015) and the *Fermi*-LAT 3FGL gamma-ray source catalog (Acero et al. 2015) are shown in cyan and red, respectively. Right panel: *AGILE* gamma-ray lightcurve above 100 MeV on the TXS 0506 +059 position, in the days before and after the T_0 of the IceCube IC-170922 event. In red, the corresponding *Fermi*-LAT lightcurve from the same position, obtained with the *Fermi*-LAT online analysis tool publicly available at the SSDC (see footnote 31).

Table 3
Gamma-Ray and Neutrino Isotropic Luminosities for the Three Sources Detected by *AGILE* Possibly Related to Three IceCube HESE/EHE Neutrinos

AGILE Source	IceCube Event	$\nu F_\gamma(\nu)$ (erg cm^{-2} s^{-1})	$D = 10$ kpc		$z = 1$		$z = 0.3365$	
			L_γ (erg s^{-1})	L_ν (erg s^{-1})	L_γ (erg s^{-1})	L_ν (erg s^{-1})	L_γ (erg s^{-1})	L_ν (erg s^{-1})
A	IC-160731	6.9×10^{-11}	8.2×10^{35}	2.2×10^{36}	2.6×10^{46}	6.8×10^{46}	...	...
B	IC-170321	7.5×10^{-11}	9.0×10^{35}	2.2×10^{36}	2.8×10^{46}	6.8×10^{46}	...	...
C	IC-170922	8.6×10^{-11}	...	...	...	...	3.2×10^{46}	6.8×10^{46}

Note. Gamma-ray luminosities are estimated over a time interval of about ±1 week around T_0; for neutrino luminosities, an active source period of six months is assumed. For Sources A and B, two possible values of distance are considered: $D = 10$ kpc, for a typical Galactic object, and redshift $z = 1$, for an extragalactic one (a standard $H_0 = 70$, $\Omega_M = 0.3$, $\Omega_\Lambda = 0.7$ cosmology has been used here for the calculation of the corresponding luminosity distance.). For Source C, only the estimated redshift of TXS 0506+059 ($z = 0.3365$) (Paiano et al. 2018) has been used for the calculation.

gamma-ray component peaking at MeV/sub-GeV due to the reprocessing of the VHE photons emitted by pion decay.

The detection of the gamma-ray Source B within the IC-170321 error box is interesting. Its position is close to the Galactic plane with no clear extragalactic known gamma-ray counterpart. This source might be considered to belong to a class of neutrino sources associated with a sub-dominant population of IceCube events apparently aligned near the Galactic plane (Halzen et al. 2017). Future observations will explore this very interesting possibility related to hidden compact objects in our Galaxy. We note that *Fermi*-LAT placed only a 95% c.l. u.l. on the gamma-ray emission above 100 MeV over an interval of one week just before T_0 (Buson et al. 2017). Similar cases of *AGILE* sources, both transient and steady, not confirmed by *Fermi*-LAT have been detected in the past (Pittori et al. 2009; Verrecchia et al. 2013; Bulgarelli et al. 2018). Several reasons can explain these discrepancies: source variability; different spectral response of the instruments; source visibility/exposure due to the different observing modes; event classification algorithms; background model (especially important for sources near the Galactic plane). All these factors may become important for relatively short gamma-ray transients (with duration of a few days) at the level of 4σ above the background.[35]

This is the first time that evidence of multiple gamma-ray sources in close spatial and temporal coincidence with cosmic neutrinos has been presented. *AGILE* continues to monitor the gamma-ray sky and to react to IceCube alerts. More simultaneous neutrino and gamma-ray events are needed to strengthen the correlation indicated in the current *AGILE* data analysis. From our analysis, different classes of neutrino sources should be considered. Continuous blazar monitoring is needed to confirm the association of BL Lac-type sources as in the case of our Source C and, in principle, Galactic sources should be also taken into account and included in future searches.

Future studies of neutrino and gamma-ray sources need sensitive detectors and space missions able to reveal transient episodes occurring in the MeV/sub-GeV energy band. The *e-ASTROGAM* space mission (De Angelis et al. 2017) has been

[35] The non-detection of the *AGILE* Source A by *Fermi*-LAT was explained by very poor visibility of the IC-160731 sky region in the days near T_0 (Lucarelli et al. 2017b).

proposed as well as the mission *AMEGO*, which is in an advanced state of development (McEnery 2017). They can accomplish this task in the 2030s along with the upgraded neutrino experiment IceCube-Gen2 (The IceCube-Gen2 Collaboration et al. 2015) and the new generations of gamma-ray and neutrino telescopes such as CTA and KM3NET (Acharya et al. 2013; Adrián-Martínez et al. 2016).

AGILE is an ASI space mission developed with scientific and programmatic support from INAF and INFN. Research partially supported through the ASI grant No. I/028/12/2. We thank ASI personnel involved in the operations and data center of the *AGILE* mission. Part of this work is based on archival data, software or online services provided by the Space Science Data Center (SSDC)—ASI. It is also based on data and/or software provided by the High Energy Astrophysics Science Archive Research Center (HEASARC), which is a service of the Astrophysics Science Division at NASA/GSFC and the High Energy Astrophysics Division of the Smithsonian Astrophysical Observatory. This research has also made use of the SIMBAD database and the VizieR catalog access tool, operated at CDS, Strasbourg, France.

Software: AGILE scientific analysis software (BUILD 21 Chen et al. 2011), XIMAGE.

Appendix A
Estimation of the FAR for *AGILE*-GRID in Spinning Mode

To evaluate the probability of finding an *AGILE* gamma-ray detection above 100 MeV in random coincidence with a candidate IceCube HESE/EHE astrophysical neutrino, we have estimated a FAR for the *AGILE*-GRID data using the whole database of QL detections hosted at the *AGILE* Data Center.

Every day an automatic *AGILE* QL procedure searches for gamma-ray transients above 100 MeV over the whole accessible sky (Bulgarelli et al. 2014). The *AGILE* QL has run since 2009 November, the start of the spinning observation mode, over predefined data time intervals of 48 hr. Given the *AGILE* effective area and sensitivity, these collecting time intervals are the most appropriate to accumulate enough statistics and to maximize the signal-to-noise ratio in spinning mode.

A blind search for gamma-ray transients is first applied to the data either using the XIMAGE detect algorithm or the so-called *spotfinder* method (Bulgarelli et al. 2014). Then, counts, exposure and diffuse background model maps, centered at the excess positions found previously, are produced using the tasks of the *AGILE* software, and eventually the count excess is evaluated against the expected background counts using the *AGILE* ML fit procedure (Bulgarelli et al. 2012).[36] All the gamma-ray detections and their ML best-estimate parameters (source significance as the square root of the ML test statistic ($\sqrt{\mathrm{TS}}$), gamma-ray flux and source location) of each candidate source are then stored in the QL detection database.

Bulgarelli et al. (2012) assessed the *AGILE* ML method, computing the chance probability to get a gamma-ray detection with a significance above a certain threshold, both for an empty extragalactic field and crowded Galactic fields. In our study, we need to extend that work in order to statistically determine the chance probability to have an *AGILE* detection above a certain threshold of $\sqrt{\mathrm{TS}}$ (over a 2 day time interval) *in temporal and spatial coincidence* with an IceCube neutrino event, having a localization error of the order of 1° in radius.

Practically, to determine the FAR for the *AGILE*-GRID data integrated over a 2 day interval, we proceed as follows:

1. a sky position in a relatively empty region of the *AGILE* gamma-ray sky is considered and, using the QL database, the number of gamma-ray detections above a certain value of $\sqrt{\mathrm{TS}}$ within a circular region of 20° in radius, centered at the chosen position, is counted;
2. the observed $\sqrt{\mathrm{TS}}$ counting frequency is divided by the number of 1.°5-radius pixels[37] contained in the sky region under evaluation;
3. the $\sqrt{\mathrm{TS}}$ counting frequency *per pixel* is divided by the *AGILE* livetime computed from the beginning of the spinning mode (MJD = 55139.5).

Since our minimum "time unit" is the 2 day integration time of the QL detections, the *AGILE* livetime is expressed as the number of 2 day "good" maps generated since MJD = 55139.5, i.e., having sufficient and uniform exposure to allow a reliable ML source parameter estimation.

In this way, we basically end with a FAR for an *AGILE* QL detection normalized to the solid angle subtended by a cone with half-aperture of 1.°5 (i.e., the database search radius) and to the duration time of the QL maps. This FAR, expressed in units of 2 day maps and unit solid angle, can be then used to evaluate the probability of an accidental detection closed both in time and in space with an external event like the IceCube neutrinos.

The number of *2 day good maps* varies according to the sky position considered, due both to the spacecraft rotation mode, in which the solar panels have to be kept fixed toward the Sun, and the seasonal variation of the Sun/anti-Sun exclusion regions due to the Earth orbital motion.[38] Figure 6, left panel, shows a Hammer–Aitoff projection in Galactic coordinates of the overall *AGILE* exposure (in cm^2 s), covering the period 2009 November–2017 September (MJD = 55139.5–58026.5). The regions around the ecliptic poles are the most exposed, while the exposure along the ecliptic plane is affected by the apparent motion of the Sun/anti-Sun exclusion regions.

The total *AGILE* livetime for the whole spinning period of almost 8 yr, expressed in terms of total number of 2 day good maps, ranges from around 1000 for the regions near the ecliptic poles down to around 200 for the less exposed sky positions on the ecliptic plane.[39] For the FAR calculation, we considered a relatively empty region of brilliant gamma-ray sources placed near the south ecliptic pole (position 1 in Figure 6, left panel). For this position, the number of 2 day good maps amounts to 1000. The value of FAR estimated on position 1 can be applied to the estimation of the false alarm probability in case of an *AGILE* QL detection consistent with an IceCube HESE/EHE

[36] For unknown sources, a simple power-law spectral model with an index equal to −2.1 is usually assumed for the ML best-fit estimate procedure.

[37] Such a pixel size is equal to the search cone radius used for the QL database scanning, which has been optimized according to the mean *AGILE* angular resolution in the 100 MeV–1 GeV energy band.

[38] On average, the exclusion regions pass over the same sky position almost every three months.

[39] The number of 2 day good maps accumulated over the whole spinning period for the two positions considered has been estimated using the *AGILE* online interactive analysis tool based on the *AGILE*-GRID Level-3 (LV3) archive of pre-computed counts, exposure, and diffuse background emission maps (available at: http://www.asdc.asi.it/mmia/index.php?mission=agilelv3mmia).

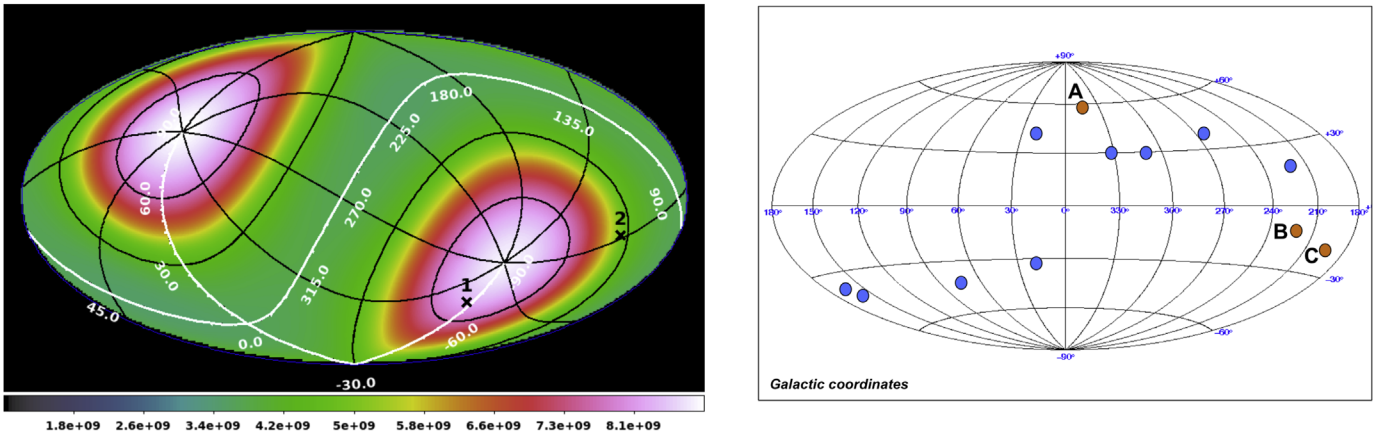

Figure 6. Left panel: Hammer–Aitoff projection, in Galactic coordinates, of the total *AGILE* gamma-ray exposure (in cm^2 s) accumulated since the beginning of the spinning observation mode (MJD = 55139.5) up to the end of 2017 September (MJD = 58026.5). The overlaid grid defines the ecliptic coordinate system. Due to the fixed orientation of the solar panels toward the Sun, the regions around the ecliptic poles are the most exposed, while the exposure along the ecliptic plane is affected by the apparent motion of the Sun/anti-Sun exclusion regions. Positions labeled as 1 and 2 have been used to estimate the false alarm rate for the *AGILE*-GRID detections over 2 day time intervals. Right panel: distribution, in a Hammer–Aitoff projection in Galactic coordinates, of the reconstructed arrival directions of the IceCube HESE/EHE neutrino events published up to 2018 August. A, B, and C indicate the three events with an *AGILE* potential gamma-ray counterpart.

event lying well above the Galactic plane (with Galactic latitude $|b| \geqslant 20^\circ$).

Since *AGILE* Sources B and C described in the main text are consistent with two IceCube events located nearer the Galactic plane ($b = -10.75$ and -19.56 (deg), respectively), to estimate the chance correlation for this region we considered a 20° region centered at Galactic coordinates l, b = (217.0, −15) (deg) (position 2 in Figure 6, left panel). Due to higher diffuse gamma-ray emission near the plane, the FAR for this region resulted to be roughly 30% higher than the value obtained at higher or lower Galactic latitudes, ending in a slightly higher value of the post-trial false alarm probability P_i for the two events, as shown in Table 1.

We notice that the FAR (and the false alarm probability) can be overestimated by 20%–30% due to the presence of an unsubtracted non-Poissonian component of *real* gamma-ray transients from unknown sources occurring in the extraction sky region.

Appendix B
IceCube HESE/EHE Events Announced since 2016 April

Table 4 shows all the IceCube HESE/EHE events published up to 2018 August. Since 2016 April, these events have been announced through the GCN/AMON notice circuit (Aartsen et al. 2017c), usually followed by a GCN Circular reporting the results of a further refined data analysis which provides improved reconstructed neutrino arrival directions and position uncertainties.

Along with the IceCube event ID, the table shows:

1. the neutrino event time (in UT and MJD date);
2. the event classification (HESE or EHE);
3. the best-fit reconstructed neutrino arrival direction in equatorial coordinates (J2000) and its uncertainty;
4. the corresponding Galactic coordinates l and b;
5. the GCN Circular number reporting about the refined analysis (if available).

Where available, the table shows the refined arrival direction published in the GCN Circular.

Event numbered 34032434 has been rejected after refined analysis (IceCube Collaboration 2017) while events 65274589 and 32674593 were considered consistent with rare atmospheric muon background events (Blaufuss 2017b, 2017c) and, thus they were not considered in our analysis.

Figure 6, right panel, shows the distribution of all IceCube events in a Hammer–Aitoff projection of the sky in Galactic coordinates. All events appear well above the Galactic plane, except for one case (IC-170321) which shows a Galactic latitude of $-10.^\circ75$. The three neutrino events with an *AGILE* possible transient counterpart, A, B, and C, are shown in orange.

Table 4
Public IceCube HESE/EHE Alerts Published through the GCN/AMON and GCN Circular Network, and Their Main Identification Parameters

Event ID	Date Time (UT)	MJD (days)	Event Class	R.A. (J2000) (deg)	Decl. (J2000) (deg)	Position Uncertainty (arcmin)	l (deg)	b (deg)	GCN Circ. #
67093193 (IC-160427)	16/04/27 05:52:32.00	57505.245	HESE	240.57	9.34	36 (90% c.r.)	20.69	41.68	19363
6888376 (IC-160731)	16/07/31 01:55:04.00	57600.079	HESE/EHE	214.544	−0.3347	45 (90% c.r.)	343.68	55.52	…
26552458 (IC-160806)	16/08/06 12:21:33.00	57606.515	EHE	122.81	−0.8061	34 (50% c.r.)	223.07	17.29	19787
58537957 (IC-160814)	16/08/14 21:45:54.00	57614.907	HESE	199.31	−32.0165	89.4 (90% c.r.)	309.28	30.54	…
38561326 (IC-161103)	16/11/03 09:07:31.12	57695.38	HESE	40.8252	12.5592	66 (90% c.r.)	160.90	−41.92	…
80127519 (IC-161210)	16/12/10 20:06:40.31	57732.838	EHE	46.5799	14.98	60 (50% c.r.)	164.89	−36.67	…
65274589 (IC-170312)[a]	17/03/12 13:49:39.83	57824.576	HESE	305.15	−26.61	±30 in R.A. ±30 in decl. (90% PSF)	16.50	−30.40	20857
80305071 (IC-170321)	17/03/21 07:32:20.69	57833.314	EHE	98.3	−15.02	±72 in R.A. ±72 in decl. (90% PSF)	224.42	−10.75	20929
32674593 (IC-170506)[a]	17/05/06 12:36:55.80	57879.526	HESE	221.8	−26	±180 in R.A. ±120 in decl. (90% PSF)	332.95	30.03	21075
50579430 (IC-170922)	17/09/22 20:54:30.43	58018.871	EHE	77.43	5.72	−48/+78 in R.A. −24/+42 in decl. (90% PSF)	195.42	−19.56	21916
56068624 (IC-171015)	17/10/15 01:34:30.06	58041.066	HESE	162.86	−15.44	−102/+156 in R.A. −120/+96 in decl. (90% PSF)	264.96	38.43	22016
34032434 (IC-171028)[b]	17/10/28 08:28:14.81	58054.353	HESE	275.076	34.5011	…	61.96	20.95	22065
17569642 (IC-171106)[c]	17/11/06 18:39:39.21	58063.778	EHE	340.0	7.4	−30/+42 in R.A.−15/+21 in decl. (90% PSF)	75.51	−43.05	22105

Notes.
[a] Possibly consistent with rare atmospheric muon background event.
[b] Event candidate retracted in GCN Circular #22065.
[c] Event consistent with being produced by a neutrino with energy in excess of 1 PeV.

ORCID iDs

F. Lucarelli https://orcid.org/0000-0002-6311-764X
M. Tavani https://orcid.org/0000-0003-2893-1459
G. Piano https://orcid.org/0000-0002-9332-5319
A. Bulgarelli https://orcid.org/0000-0001-6347-0649
I. Donnarumma https://orcid.org/0000-0002-4700-4549
F. Verrecchia https://orcid.org/0000-0003-3455-5082
C. Pittori https://orcid.org/0000-0001-6661-9779
L. A. Antonelli https://orcid.org/0000-0002-5037-9034
P. Caraveo https://orcid.org/0000-0003-2478-8018
M. Cardillo https://orcid.org/0000-0001-8877-3996
P. W. Cattaneo https://orcid.org/0000-0001-6877-6882
V. Fioretti https://orcid.org/0000-0002-6082-5384
P. Giommi https://orcid.org/0000-0002-2265-5003
F. Longo https://orcid.org/0000-0003-2501-2270
S. Mereghetti https://orcid.org/0000-0003-3259-7801
A. Ursi https://orcid.org/0000-0002-7253-9721
S. Vercellone https://orcid.org/0000-0003-1163-1396
V. Vittorini https://orcid.org/0000-0002-1208-8818

References

Aartsen, M. G., Abraham, K., Ackermann, M., et al. 2013, Sci, 342, 1242856
Aartsen, M. G., Abraham, K., Ackermann, M., et al. 2015, PhRvL, 115, 081102
Aartsen, M. G., Abraham, K., Ackermann, M., et al. 2017a, ApJ, 835, 151
Aartsen, M. G., Abraham, K., Ackermann, M., et al. 2017b, ApJ, 835, 45
Aartsen, M. G., Ackermann, M., Adams, J., et al. 2017c, APh, 92, 30
Aartsen, M. G., Ackermann, M., Adams, J., et al. 2018a, Sci, 361, eaat1378
Aartsen, M. G., Ackermann, M., Adams, J., et al. 2018b, Sci, 361, 147
Acero, F., Ackermann, M., Ajello, M., et al. 2015, ApJS, 218, 23
Acharya, B. S., Actis, M., Aghajani, T., et al. 2013, APh, 43, 3
Adrián-Martínez, S., Ageron, M., Aharonian, F., et al. 2016, JPhG, 43, 084001
Ahlers, M., Bai, Y., Barger, V., & Lu, R. 2016, PhRvD, 93, 013009
Albert, A., André, M., Anghinolfi, M., et al. 2017, PhRvD, 96, 082001
Anchordoqui, L. A., Barger, V., Cholis, I., et al. 2014, JHEAp, 1, 1
Becker Tjus, J., Eichmann, B., Halzen, F., Kheirandish, A., & Saba, S. M. 2014, PhRvD, 89, 123005
Bednarek, W. 2005, ApJ, 631, 466
Blaufuss, E. 2017a, GCN Circ., 20929
Blaufuss, E. 2017b, GCN Circ., 20857
Blaufuss, E. 2017c, GCN Circ., 21075, https://gcn.gsfc.nasa.gov/other/icecube_170506A.gcn3
Bulgarelli, A., Chen, A. W., Tavani, M., et al. 2012, A&A, 540, A79
Bulgarelli, A., Fioretti, V., Parmiggiani, N., et al. 2018, ApJ, submitted
Bulgarelli, A., Trifoglio, M., Gianotti, F., et al. 2014, ApJ, 781, 19
Buson, S., Kocevski, D., & Ciprini, S. 2017, GCN Circ., 20971
Chang, Y.-L., Arsioli, B., Giommi, P., & Padovani, P. 2017, A&A, 598, A17
Chang, Y.-L., Arsioli, B., Giommi, P., Padovani, P., & Brandt, C. 2018, A&A, submitted
Chen, A. W., Bulgarelli, A., Contessi, T., et al. 2011, GRID Scientific Analysis–USER MANUAL, http://agile.asdc.asi.it
Connaughton, V., Burns, E., Goldstein, A., et al. 2016, ApJL, 826, L6
De Angelis, A., Tatischeff, V., Tavani, M., et al. 2017, ExA, 44, 25
Gaisser, T. K., Halzen, F., & Stanev, T. 1995, PhR, 258, 173
Halzen, F. 2017, NatPh, 13, 232
Halzen, F., Kheirandish, A., & Niro, V. 2017, APh, 86, 46
IceCube Collaboration 2017, GCN Circ., 22065
Keivani, A. 2017, IceCube-170321A: Swift-XRT Observations
Kopper, C., & Blaufuss, E. 2017, GCN Circ., 21916
Kotera, K., Allard, D., Murase, K., et al. 2009, ApJ, 707, 370
Lamastra, A., Menci, N., Fiore, F., et al. 2017, A&A, 607, A18
Loeb, A., & Waxman, E. 2006, JCAP, 5, 003
Lucarelli, F., Piano, G., Pittori, C., et al. 2017a, ATel, 10801
Lucarelli, F., Pittori, C., Verrecchia, F., et al. 2014, ATel, 6457
Lucarelli, F., Pittori, C., Verrecchia, F., et al. 2017b, ApJ, 846, 121
Mannheim, K. 1995, APh, 3, 295
Massaro, E., Maselli, A., Leto, C., et al. 2015, Ap&SS, 357, 75
McEnery, J. E. 2017, AAS/High Energy Astrophysics Division, 16, 103.13
Mészáros, P. 2017, ARNPS, 67, 45
Murase, K., Inoue, S., & Nagataki, S. 2008, ApJL, 689, L105
Ojha, R., Carpenter, B., Becerra, J., et al. 2014, ATel, 6425
Padovani, P., Giommi, P., Resconi, E., et al. 2018, MNRAS, 480, 192
Padovani, P., Resconi, E., Giommi, P., Arsioli, B., & Chang, Y. L. 2016, MNRAS, 457, 3582
Paiano, S., Falomo, R., Treves, A., & Scarpa, R. 2018, ApJL, 854, L32
Pittori, C., Verrecchia, F., Chen, A. W., et al. 2009, A&A, 506, 1563
Resconi, E., Coenders, S., Padovani, P., Giommi, P., & Caccianiga, L. 2017, MNRAS, 468, 597
Sabatini, S., Donnarumma, I., Tavani, M., et al. 2015, ApJ, 809, 60
Sahakyan, N., Piano, G., & Tavani, M. 2014, ApJ, 780, 29
Savchenko, V., Santander, M., Keivani, A., et al. 2017, GCN Circ., 20937
Svinkin, D., Golenetskii, S., Aptekar, R., et al. 2017, GCN Circ., 20973
Tanaka, Y. T., Buson, S., & Kocevski, D. 2017, ATel, 10791
Tavani, M., Barbiellini, G., Argan, A., et al. 2009, A&A, 502, 995
Tavecchio, F., Righi, C., Capetti, A., Grandi, P., & Ghisellini, G. 2018, MNRAS, 475, 5529
The IceCube-Gen2 Collaboration, Aartsen, M. G., et al. 2015, arXiv:1510.05228
Verrecchia, F., Pittori, C., Chen, A. W., et al. 2013, A&A, 558, A137
Vissani, F. 2006, APh, 26, 310
Wang, X., & Loeb, A. 2016, JCAP, 12, 012